PNAS
www.pnas.org

Supplementary Information for

Wnt signaling recruits KIF2A to the spindle to ensure chromosome congression and alignment during mitosis.

Anja Bufe[1], Ana García del Arco[1], Magdalena Hennecke[2], Anchel de Jaime-Soguero[1], Matthias Ostermaier[3], Yu-Chih Lin[2], Anja Ciprianidis[1], Janina Hattemer[1], Ulrike Engel[1,4], Petra Beli[3], Holger Bastians[2] and Sergio P. Acebrón[1,*]

Correspondence to: Sergio P. Acebrón
Email: sergio.acebron@cos.uni-heidelberg.de

This PDF file includes:

1. Supplemental Figures S1 to S7
2. Supplemental Methods
3. References for the supplemental methods and figures (Supplemental References)

Other supplementary materials for this manuscript include the following:

Supplemental dataset 1

1. Supplemental Figures

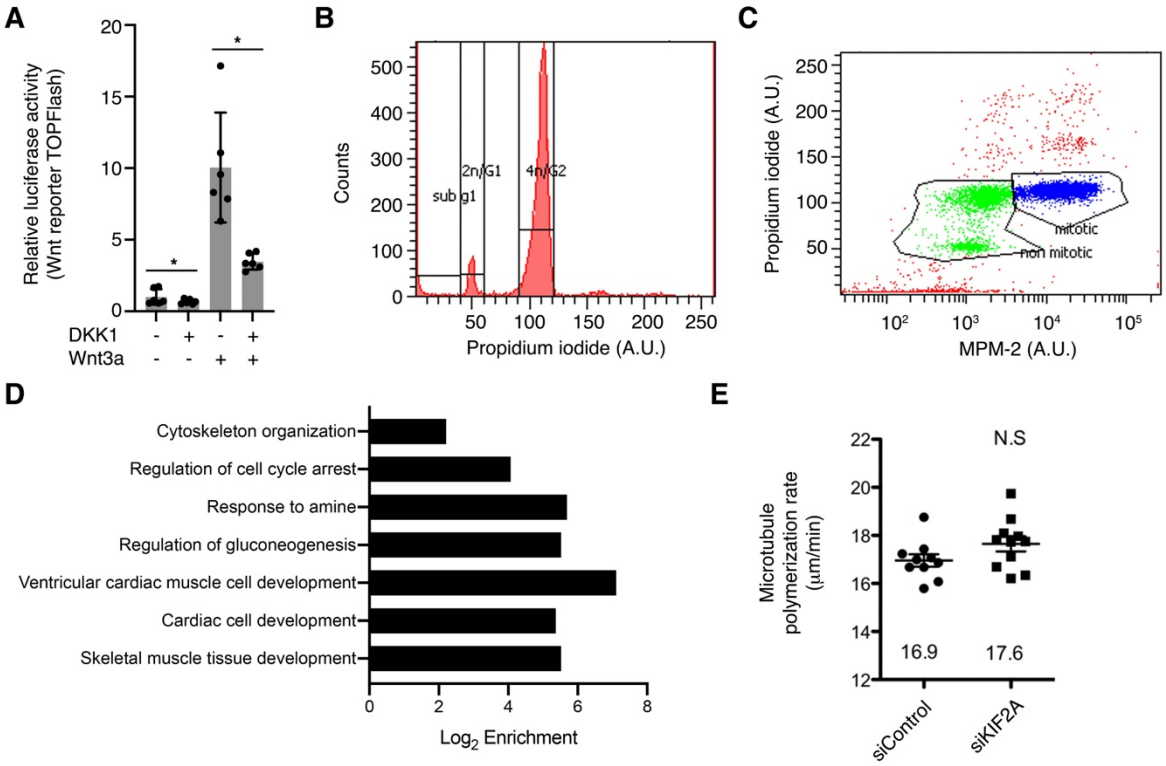

Figure S1 – Controls for the analysis of Wnt signaling and KIF2A in mitosis

A, Wnt reporter assays in RPE1 cells showing the activity of DKK1 and Wnt3a conditioned media used in these studies. Data is displayed as mean ± SD of 6 biological replicates. **B,C,** FACS cell cycle profiles of RPE1 cells that were synchronized as described in Figure 1A and the methods. Mitotic cells (PI = 4n; MPM-2 positive) are shown in blue and represent ~66% of the population. **D,** Gene ontology enrichment (Log_2) of DKK1 target proteins (fold change > 2 in each experiment) from Figure 1A,B. **E,** Measurements of microtubule plus end assembly rates in EB3-EGFP transiently transfected RPE1 cells during mitosis after siRNA-mediated knockdown of KIF2A (20 microtubules/cells, n = 10 cells).

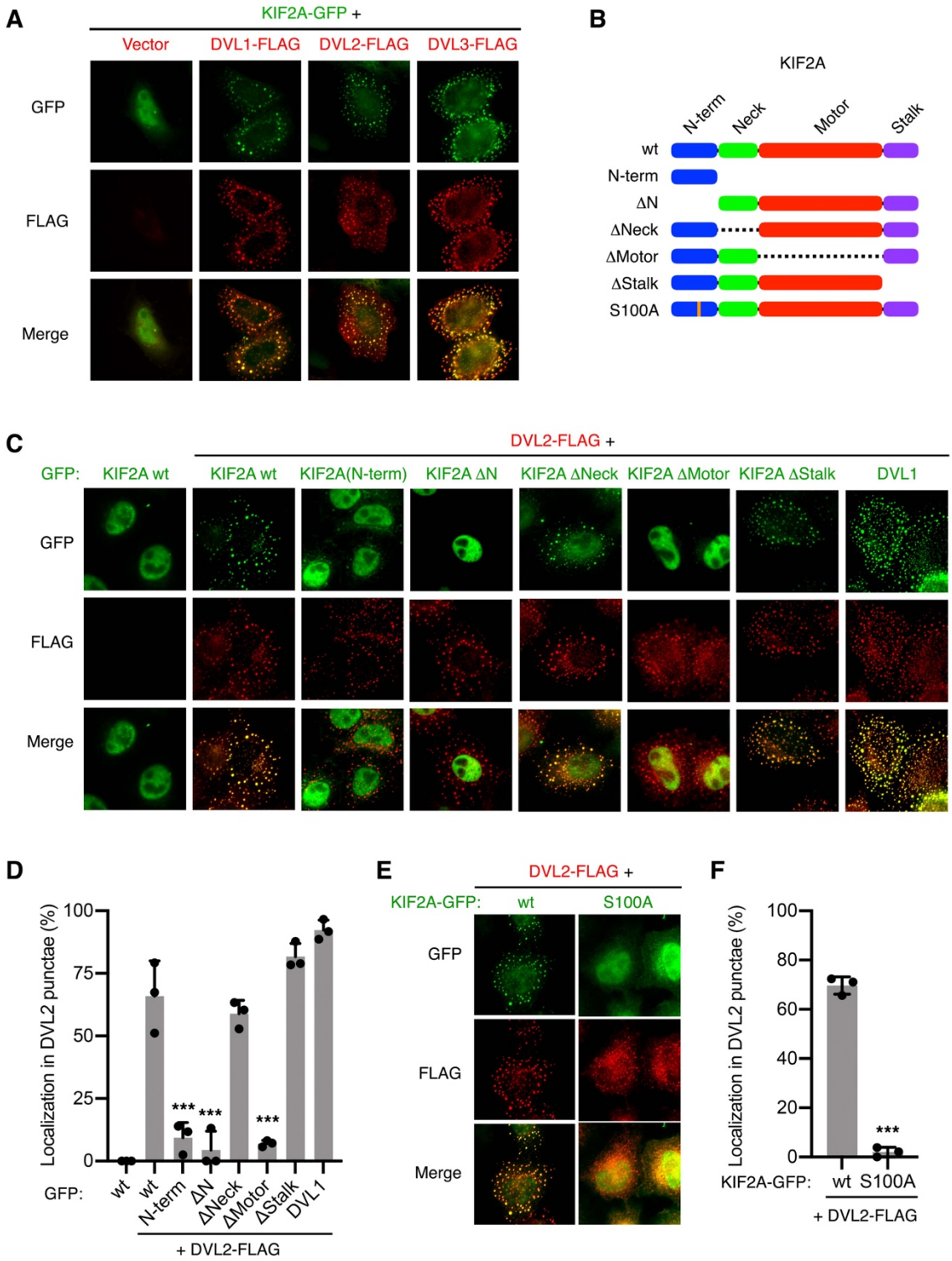

Figure S2 – KIF2A is recruited by Dishevelled through its N-terminal and motor domains

A,C,E, Representative immunofluorescence microscopy images from n ≥ 3 independent experiments showing HeLa cells transfected with the indicated FLAG- or GFP-tagged constructs. **B,** Scheme showing the KIF2A constructs used in (**C-F**). **D,F,** Bar plots showing the percentage of cells with strong co-localization of GFP-tagged constructs and DVL2-FLAG from (**C,E**). Data is displayed as mean ± SD from 3 independent experiments with n ≥ 20 cells/condition in each experiment.

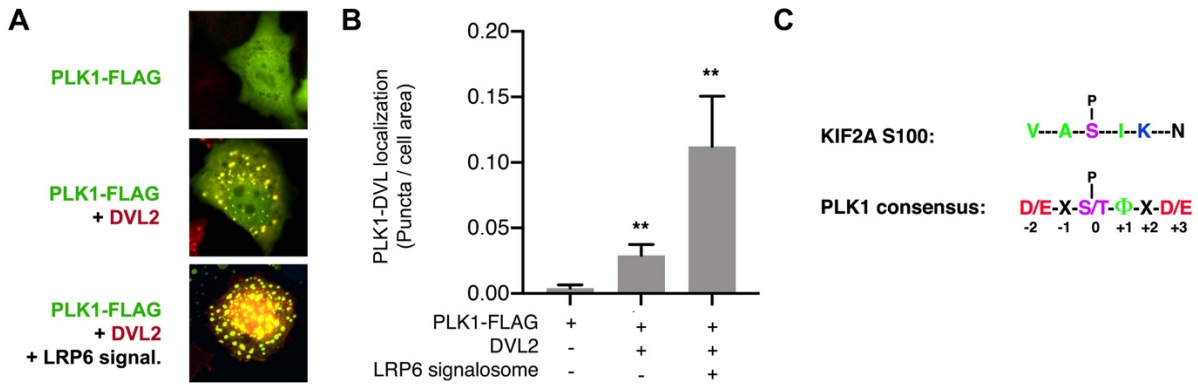

Figure S3 – PLK1 recruitment to Dishevelled is promoted by the LRP6 signalosome

A, Representative immunofluorescence microscopy images from n = 2 independent experiments showing HeLa cells transfected with PLK1-FLAG and empty vector, DVL2 or DVL2 and the LRP6 signalosome (Wnt3a/LRP6/FZD8/AXIN1). **B,** Bar plots showing the number of PLK1 positive interphase puncta relative to the size of the cell from (**A**). Data is displayed as mean ± SD from one of two independent experiments with n ≥ 14 cells/condition. **C,** Scheme showing the phospho-site of KIF2A that was identified in our MS screen (Figure 1) and the common PLK1 consensus phosphorylation motif (1). For optimal phosphorylation by PLK1, a Serine or Threonine (S/T at position 0) should be flanked by an acidic amino acid two positions preceding the phospho-site (D/E at position -2), and a hydrophobic amino acid (Φ at position +1) followed by an acidic amino acid (D/E at position +3) proximate to the site.

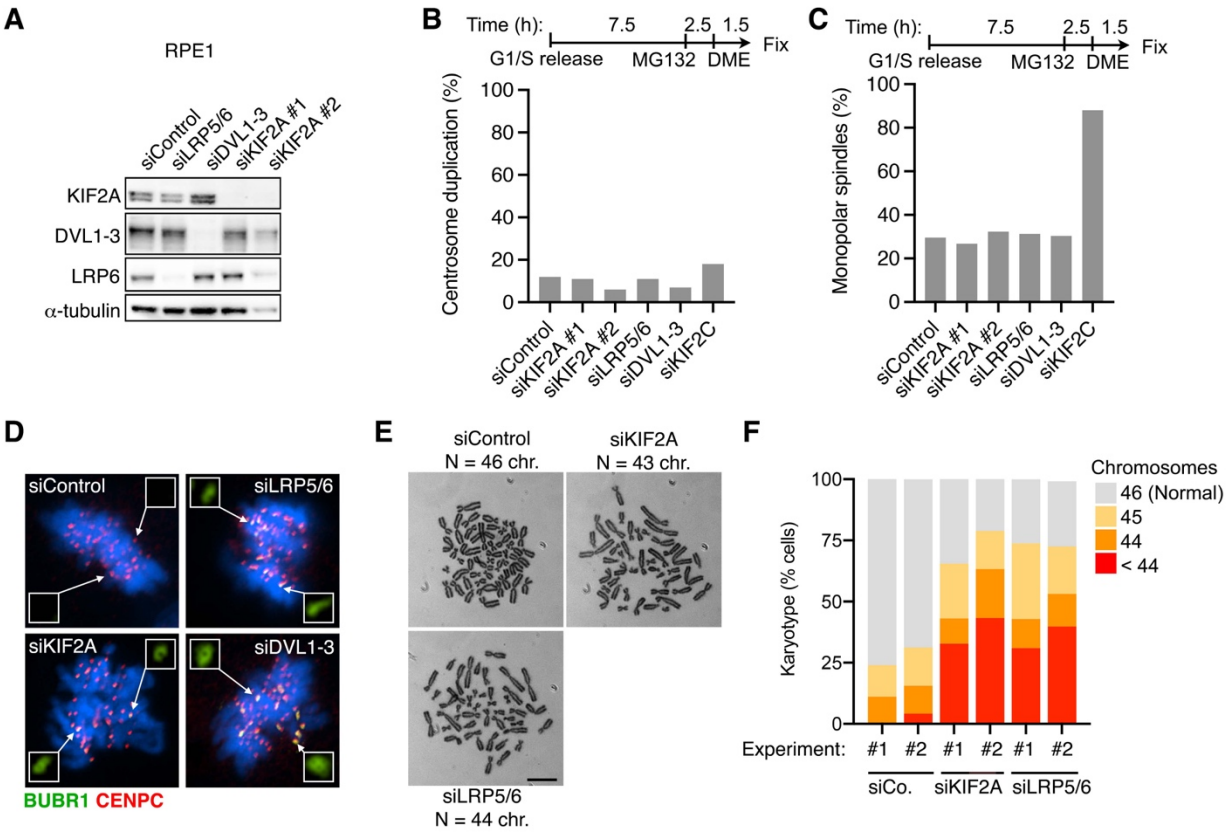

Figure S4 – Investigation of causes and consequences of chromosomal misalignment

A, Western blots from RPE1 cells showing the knockdown efficiency of the siRNAs used in Figure 3. **B,C,** Quantification of supernumerary centrosomes **(B)** and monopolar spindles **(C)** in HeLa cells transfected with the indicated siRNAs. Cells were synchronized and treated with dimethylenastron (DME, Eg5 inhibitor) in metaphase as described in the methods. Data represent n = 100 cells from 2 independent experiments. **D,** Representative immunofluorescence microscopy images of mitotic RPE1 cells transfected with the indicated siRNAs. CENPC marks the kinetochores and BUBR1 highlights the activation of the spindle assembly checkpoint (SAC) by misaligned chromosomes. **E,F,** Chromosome number variability of RPE1 cells transfected with the indicated siRNAs every 5 days and grown over 30 generations. In (**E**), representative examples of metaphase chromosome spreads, including normal (46, siControl) and aneuploid karyotypes (siKIF2A, siLRP5/6), are displayed. The graph in (**F**) shows the proportion of cells harboring a karyotype with chromosome numbers deviating from modal of two experiments with 50 metaphase spreads per condition.

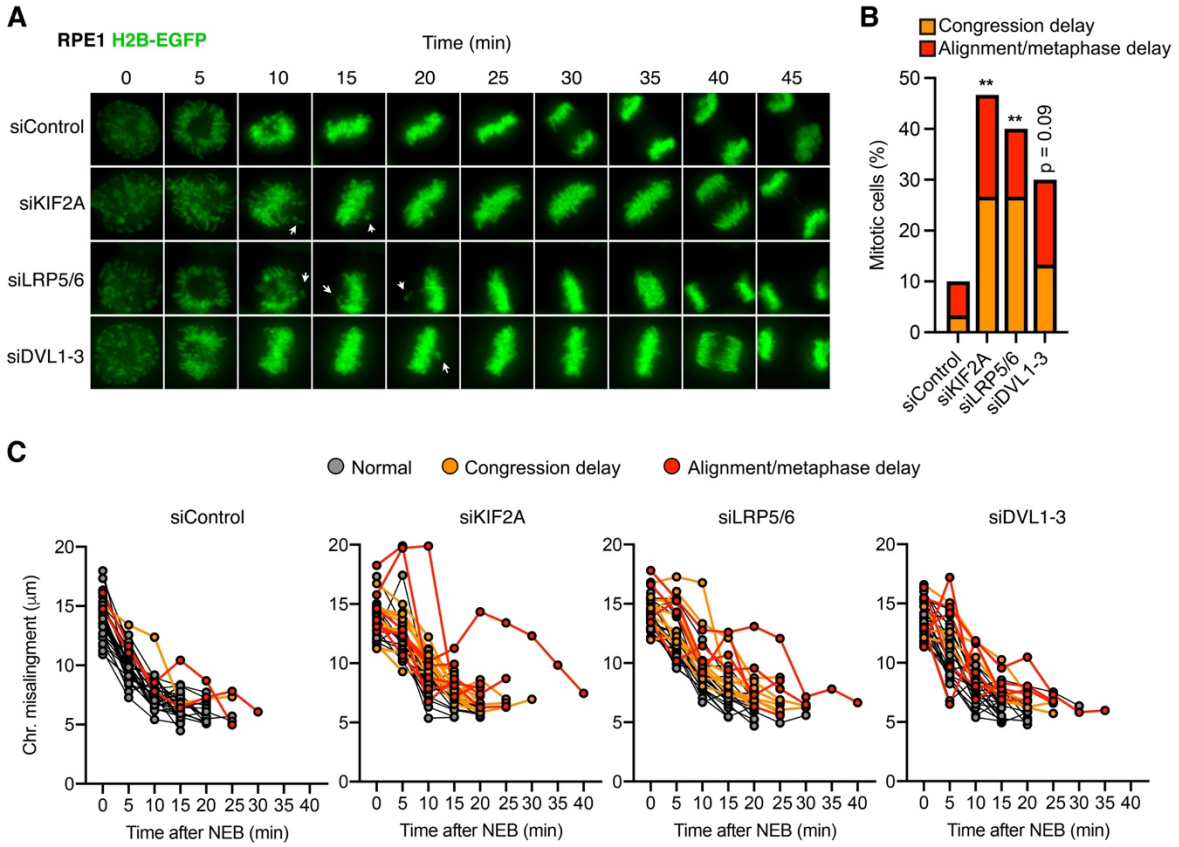

Figure S5 – Basal Wnt signaling is required for timely chromosome congression and alignment

A, Representative time lapses of mitotic RPE1 cells stably expressing H2B-EGFP, which were transfected with the indicated siRNAs. **B,C,** Analysis of congression and alignment delay from (**A**). In (C) the width covered by condensed chromosomes from the nuclear envelope breakdown (NEB) until anaphase onset is displayed for n = 25 cells per condition. Aberrant phenotypes are highlighted in orange (congression delay) and red (alignment or metaphase delay).

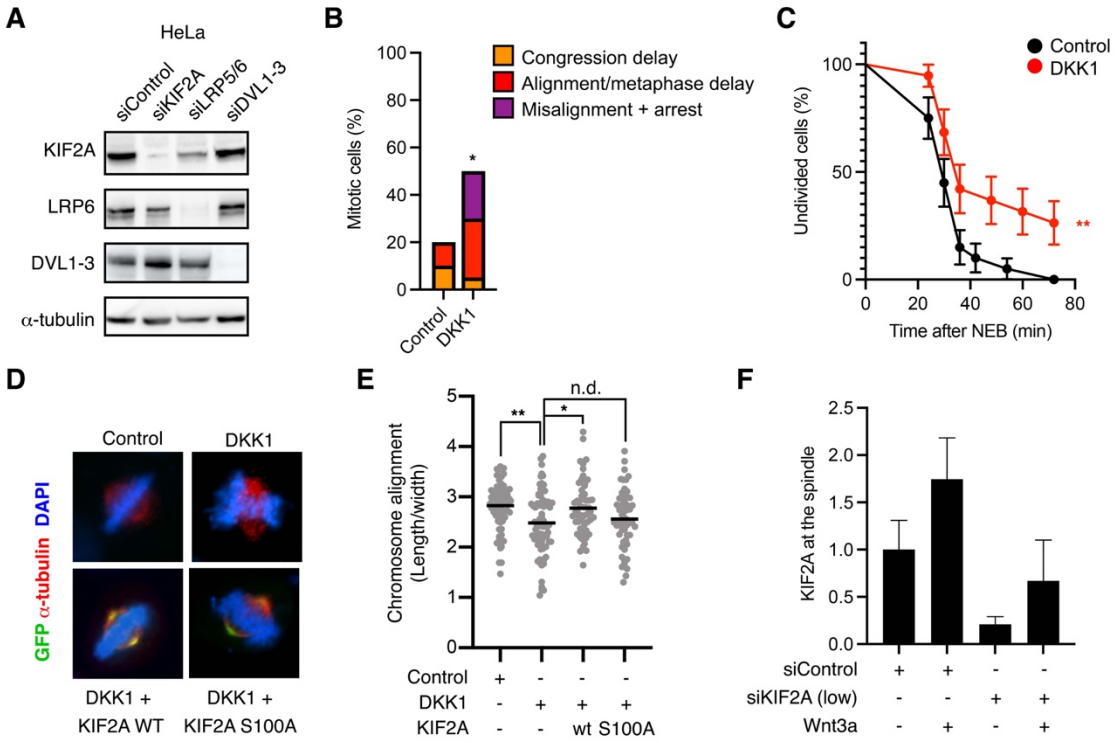

Figure S6 – Wnt promotes chromosome congression and alignment through KIF2A

A, Western blots from HeLa cells showing the knockdown efficiency of the siRNAs used in Figure 4. **B,** Analysis of congression and alignment delay in n = 20 HeLa-EB3-EGFP cells, stained with SiR-DNA and treated with control or DKK1 conditioned medium just before imaging. **C,** Analysis of mitotic progression from NEB to anaphase onset in HeLa-EB3-EGFP cells from (**B**). **D,** Representative immunofluorescence microscopy images of mitotic HeLa cells transfected with empty, EGFP-KIF2A WT or EGFP-KIF2A S100A plasmid for 24 h and treated with control or DKK1 conditioned medium for 1.5 h. **E,** Quantification of chromosome alignment from (**D**). The length occupied by the chromosomes at the metaphase plate was divided by the width towards the spindle poles in n > 49 mitotic cells per condition. The mean value is shown. **F,** Quantification of endogenous KIF2A protein levels at the mitotic spindle from figure 4H,I. Note that Wnt3a does not impact total protein levels, as shown in Figure 1L, but increases the proportion of spindle-bound KIF2A (see Figure 1J)

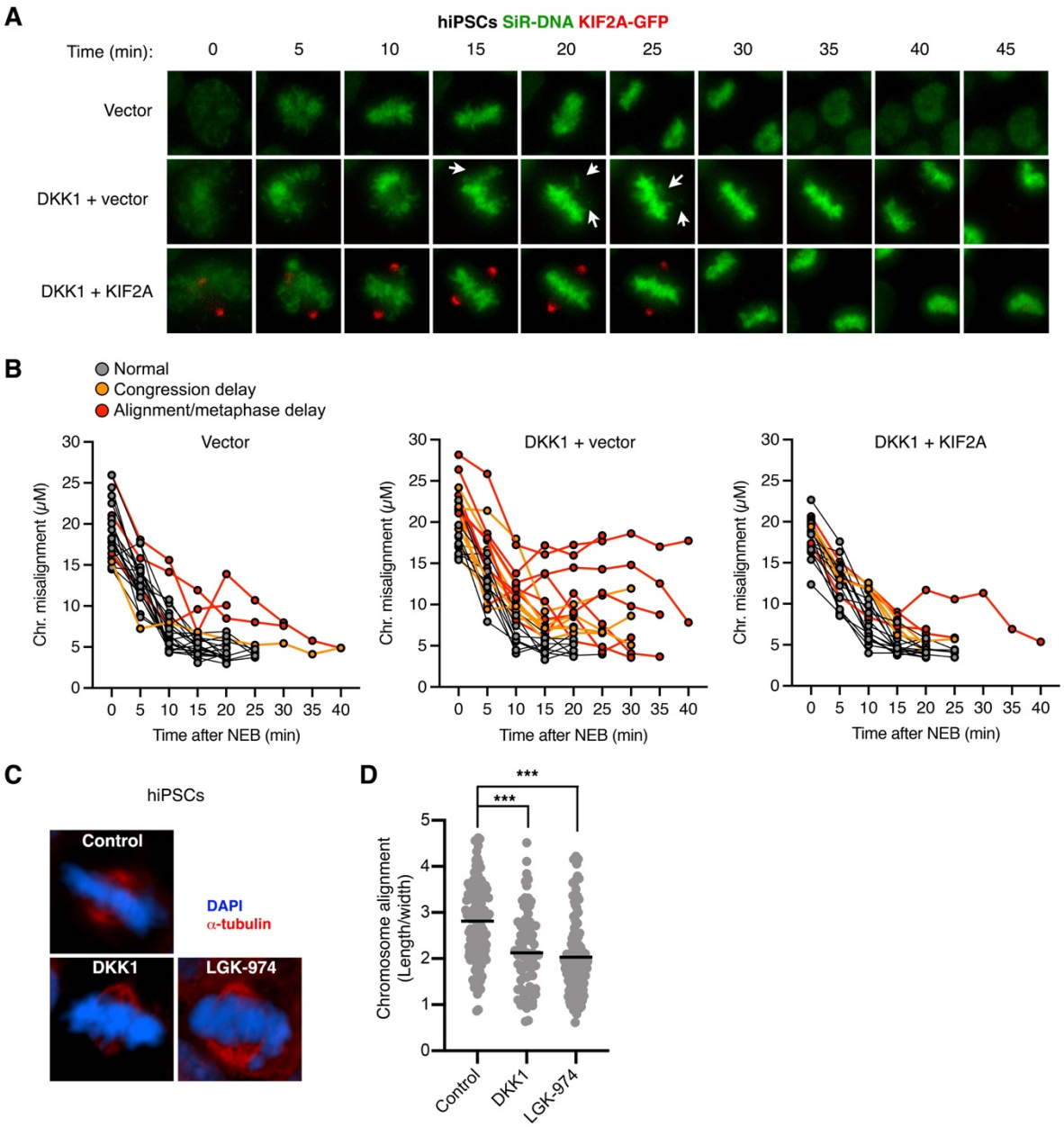

Figure S7 –Wnt signaling promotes chromosome congression and alignment through KIF2A in hiPSCs

A, Representative time lapses of mitotic hiPSCs transfected with empty vector or EGFP-KIF2A, stained with SiR-DNA and treated with control or DKK1 conditioned medium. **B,** Analysis of congression and alignment delay in n > 20 hiPSCs from (**A**). The width covered by the condensed chromosomes is shown for every single cell from NEB until anaphase. Additional analyses are shown in Figure 5D,E. **C,** Representative immunofluorescence microscopy images of mitotic hiPSCs treated with the Wnt inhibitors DKK1 and LGK-974. **D,** Quantification of chromosome alignment from **(C)**. The length occupied by the chromosomes at the metaphase plate was divided by the width towards the spindle poles in n > 85 mitotic cells per condition. The median value is indicated. Representative images and analyses of n = 4 independent experiments**.**

2. Supplemental Methods

DNA transfection and expression constructs

To generate a phospho-inactive version of the S100 site on KIF2A, the first base of the codon specifying serine (TCT) was replaced by a guanine resulting in a triplet encoding alanine (GCT), as indicated in the sequence below (Table S1). To obtain truncation mutants of the different KIF2A domains each domain was deleted by using a specific primer pair against the adjacent sites of the domain in PCR. RNAi resistant constructs of KIF2A wildtype and S100A were cloned by replacing every third base of the codons included in the siKIF2A binding sequence, without changing the encoded amino acids (Table S1).

Table S1. Primer sequences for generating the DNA constructs used in this study.

Construct	Forward primer	Reverse primer
Linearized KIF2A plasmid	TTGGACCCCCTTCACGTAGA	TTGCCTTTTGTATCTCCAT

Construct	Sequence
Oligonucleotide including S100A mutation (*in vitro* synthesized by Sigma Aldrich)	AGAGATTGACCTGGAGAGCATCTTTTCACTTAACCCTGACCT TGTTCCTGATGAAGAAATTGAACCCAGTCCAGAAACACCTCC ACCTCCAGCATCCTCAGCCAAAGTAAACAAAATTGTAAAGAA TCGACGGACTGTAGCTGCTATTAAGAATGACCCTCCTTCAAG AGATAATAGAGTGGTTGGTTCAGCACGTGCACGGCCCAGTC AATTTCCTGAACAGTCTTCCTCTGCACAACAGAATGGTAGTG TTTCAGATATATCTCCAGTTCAAGCTGCA AAAAAGGAAT

Construct	Forward primer	Reverse primer
KIF2A-ΔN (Δ1-153)	CCCCCTTCACGTAGAAAATC TAATTGTG	CATAGAATTCGAAGCTTGAG CTCG
KIF2A2-ΔNECK (Δ154-221)	CATAGGATATGTGTGTGTGT AAGAAAACG	TGAAGGGGGTCCAAATTCCT TT
KIF2A2-ΔMOTOR (Δ222-542)	ACATTAAGATATGCAAATAG GGTC	TTCATCAATAGGATCTGCTG TTG
KIF2A2-ΔSTALK (Δ543-706)	TAAGTCGACGGTACCGC	ATTAAGAGTATTTTCACAGG ATGCCATTCC
KIF2A-N (Δ154-706)	TAAGTCGACGGTACCGC	TGAAGGGGGTCCAAATTCCT TT
siRNA resistant KIF2A wildtype and KIF2A S100A	TGGAACAGAAAATAGACATT TTAACTGAACTG	GGATGGCCTCAAGTTGTGTA GCATATGAATC

Primers for qPCR

The following primer pairs were used for qPCR:

Gene	Forward primer	Reverse primer
KIF2A	AACAGCAGGTTCAAGTGGTG	TCTGAAACACTGCATGGCTC
AXIN2	AGTGCAAACTTTCGCCAACC	TGAAGGACCTGTATCCACTGTC
GAPDH	TCAAGAAGGTGGTGAAGCAGG	ACCAGGAAATGAGCTTGACAAA

MS sample preparation and analysis

RPE1 cells were cultured in either Medium or Heavy SILAC media (Cambridge Isotope Laboratories) as previously described (2) and outlined in the methods. The experiment also included Light SILAC media labeled cells, which were not used for the downstream analysis. After harvesting, cells were lysed in modified RIPA buffer (50 mM Tris pH 7.5, 650 mM NaCl, 1 mM EDTA, 1% NP-40, 0.1% sodium deoxycholate) supplemented with protease inhibitors (Complete protease inhibitor cocktail tablets, Roche Diagnostics), 1 mM sodium orthovanadate, 5 mM β-glycerophosphate, and 5 mM sodium fluoride (Sigma Aldrich). After sonication, the lysates were cleared by centrifugation at 16,000 × *g* for 15 min and protein concentrations were estimated using QuickStart Bradford Protein assay (BioRad). After combining the same amount of proteins from each label, the proteins were precipitated in fourfold excess of ice-cold acetone and subsequently re-dissolved in denaturation buffer (6 M urea, 2 M thiourea in 10 mM HEPES pH 8.0). Cysteines were reduced with 1 mM dithiothreitol (DTT) and alkylated with 5.5 mM chloroacetamide. Proteins were digested with endoproteinase Lys-C (Wako Chemicals) and sequencing grade-modified trypsin (Sigma Aldrich). Protease digestion was stopped by addition of trifluoroacetic acid to 0.5% and precipitates were removed by centrifugation. Peptides were purified using reversed-phase Sep-Pak C18 cartridges (Waters) and eluted in 50% acetonitrile. For the enrichment of phosphorylated peptides, 5 mg of peptides in binding buffer (50% acetonitrile, 6% trifluoroacetic acid in H_2O) were incubated with 10 mg of TiO_2 spheres (GL Sciences) for 1 h. The supernatant was used for a second enrichment step. The beads were washed twice in binding buffer, twice in wash buffer (0.5% TFA, 50% ACN) and subsequently peptides were eluted using elution buffer (10% NH_4OH, 25% acetonitrile in H_2O). The eluates were concentrated to remove NH_4OH and peptides were fractionated in five fractions using micro-column-based strong-cation exchange chromatography and desalted on reversed-phase C18 StageTips (3).

Peptide fractions were analyzed on a quadrupole Orbitrap mass spectrometer (Q Exactive Plus, Thermo Scientific) equipped with a UHPLC system (EASY-nLC 1000, Thermo Scientific) (4). Peptide samples were loaded onto C18 reversed phase columns (15 cm length, 75 μm inner diameter, 1.9 μm bead size) and eluted with a linear gradient from 8 to 40% acetonitrile containing 0.1% formic acid over 2 h. The mass spectrometer was operated in data dependent mode, automatically switching between MS and MS2 acquisition. Survey full-scanMS spectra (*m/z* 300–1650) were acquired in the Orbitrap. The ten most intense ions were sequentially isolated and fragmented by higher energy C-trap dissociation (HCD) (4). Peptides with unassigned charge states, as well as with charge states less than +2 were excluded from fragmentation. Fragment spectra were acquired in the Orbitrap mass analyzer.

Raw data files were analyzed using MaxQuant (development version 1.5.2.8) (5). Parent ion and MS2 spectra were searched against a database containing 92,578 human protein sequences obtained from the UniProtKB released in December 2016 using Andromeda search engine (6). Spectra were searched with a mass tolerance of 6 ppm in MS mode, 20 ppm. in HCD MS2 mode, strict trypsin specificity and

allowing up to two miscleavages. Cysteine carbamidomethylation was searched as a fixed modification, whereas cysteine modification with n-ethylmaleimide, protein N-terminal acetylation, methionine oxidation, and phosphorylation of serine, threonine, and tyrosine were searched as variable modifications. Site localization probabilities were determined by MaxQuant using the PTM scoring algorithm as described previously (5). The dataset was filtered based on posterior error probability to arrive at a false discovery rate below 1% estimated using a target-decoy approach (7). For downstream analysis, only phosphorylated peptides with a localization probability ≥ 0.75 were used. Fold-changes > 2 in both replicate experiments were considered significant.

3. Supplemental References

1. Nakajima H, Toyoshima-Morimoto F, Taniguchi E, & Nishida E (2003) Identification of a consensus motif for Plk (Polo-like kinase) phosphorylation reveals Myt1 as a Plk1 substrate. *J Biol Chem* 278(28):25277-25280.
2. Ong SE*, et al.* (2002) Stable isotope labeling by amino acids in cell culture, SILAC, as a simple and accurate approach to expression proteomics. *Mol Cell Proteomics* 1(5):376-386.
3. Weinert BT*, et al.* (2013) Lysine succinylation is a frequently occurring modification in prokaryotes and eukaryotes and extensively overlaps with acetylation. *Cell Rep* 4(4):842-851.
4. Olsen JV*, et al.* (2007) Higher-energy C-trap dissociation for peptide modification analysis. *Nat Methods* 4(9):709-712.
5. Cox J & Mann M (2008) MaxQuant enables high peptide identification rates, individualized p.p.b.-range mass accuracies and proteome-wide protein quantification. *Nat Biotechnol* 26(12):1367-1372.
6. Cox J*, et al.* (2011) Andromeda: a peptide search engine integrated into the MaxQuant environment. *J Proteome Res* 10(4):1794-1805.
7. Elias JE & Gygi SP (2007) Target-decoy search strategy for increased confidence in large-scale protein identifications by mass spectrometry. *Nat Methods* 4(3):207-214.